THE ASTROPHYSICAL JOURNAL, 309:667–673, 1986 October 15

MSH 10−53: A SUPERNOVA REMNANT INTERACTING WITH MOLECULAR CLOUDS

MARÍA TERESA RUIZ[1] AND JORGE MAY
Departamento de Astronomia, Universidad de Chile
Received 1985 October 29; accepted 1986 February 6

ABSTRACT

We present optical spectrophotometry and CO radio observations that indicate the presence of a shock expanding and interacting with the surrounding molecular clouds.

We also establish that the shock originated in a supernova explosion (probably of a massive star) occurred some 10^4 yr ago at about 2.9 kpc from us in the near side of the Carina spiral arm.

Subject headings: interstellar: molecules — nebulae: individual — nebulae: supernova remnants

I. INTRODUCTION

Recently, the study of the interaction between a supernova and a molecular cloud has become a subject of great astronomical relevance. There have been claims that such an event will induce star formation (Herbst and Assousa 1977) and supernovae are taken to be the main source of cosmic rays in molecular clouds thanks to which the coldest clouds can overcome gravitational collapse.

Good evidence of the interaction between a supernova shock wave and molecular clouds have been found in a few cases (Cornett, Chin and Knapp 1977; Scoville *et al.* 1977; Wootten 1981). Broad molecular emission lines without an associated infrared source (heating source), and abnormal chemical abundances in the shocked clouds are some of the signs of the interaction between a supernova remnant and its surrounding molecular clouds.

In this paper we present optical and CO radio observations of the remnant MSH 10−53 which indicate that it is located in the near side of the Carina spiral arm and interacting with the molecular clouds in that region.

MSH 10−53 (G284.2−1.8) was first identified as an extended radio source by Mills, Slee and Hill (1961). Later based on the spectral index at 1 GHz, $\alpha = -0.46$, Milne (1971) suggested that MSH 10−53 could be a supernova remnant, with an angular size of 23′ × 12′. Applying the Σ-D relation to the remnant, he derived a diameter of 16.9 pc and a distance of 3.5 kpc. The high polarization (5%) at 5 GHz found by Milne and Dickel (1975) in this source, is typical of supernova remnants.

This remnant is in an area of the sky ($10^h17^m51^s.6$, −58°32′55″; 1950) full of H II regions and dust belonging to the near side of the Carina spiral arm. In spite of the unfavorable location for optical detection of the remnant, a faint optical filament (Fig. 1) was found near the edge of the radio source (van den Bergh, Marscher, and Terzian 1973).

Up until now there was no spectroscopic confirmation of the possible supernova origin of the filament and its relation to the extended nonthermal radio source MHS 10−53.

II. OBSERVATIONS

a) Optical

Optical observations were made from Cerro Tololo Interamerican Observatory during 1984–1985. A plate of the optical filament (see Fig. 1) in MSH 10−53 was obtained with the PF camera of the 4 m telescope. The plate was a baked 098-04, taken through an Hα filter and with an exposure time of 2 hr.

Three long slit spectrograms (3′.5 in length) of the filament were obtained with the Cassegrain Spectrograph and a SIT Vidicon tube attached to the CTIO 1.5 m telescope. The aperture used for the extraction was 60″ by 2″.5, and its position is indicated in Figure 1.

Figure 2*a* shows a spectrogram covering the range between 3650 Å and 5130 Å with a resolution of about 10 Å; the integration time for it was 4800 s.

Figure 2*b* shows a spectrogram at the same position as above, but, covering the spectral range between 5350 Å and 6850 Å at 10 Å resolution, the integration time was 3600 s. A third spectrogram was taken covering the range between 3900 Å and 7200 Å at 15 Å resolution with an integration time of 1200 s; from this last spectrum we obtained the value of the Hα/Hβ ratio, used to correct the observed line intensities for interstellar reddening.

Reduction of the spectra was performed using the La Serena CTIO computing facilities.

Contribution from the night sky was subtracted using parts of the spectrograms where little or no emission from the remnant is present.

b) CO Observations

Observations of the 2.6 mm line of CO (^{12}CO $J = 1$–0) in the MSH 10−53 region were made, during 1984 September and October, with the 1.2 m Columbia Millimeter-Wave Telescope located at Cerro Tololo. A detailed description of the instrument has been given by Cohen (1983). At the frequency of 115 GHz (2.6 mm) the radiotelescope has an angular resolution of 8′.7 (HPBW), and the spectrometer used, a 256 channel filterbank of 0.5 MHz bandwidth per channel, provided a resolution in radial velocity of 1.3 km s^{-1} with a total velocity coverage of 332.8 km s^{-1}. Position switching was used with equal amount of time (15 s) spent on the "on" and the "off" positions until a rms noise of 0.1 K was achieved. The angular difference between the reference (off) and the source (on) position was usually less than 10° in azimuth and less than 0°.5 in elevation. The integration times were selected and updated by computer control on a real time basis. typically a 7 minute integration time was necessary to achieve a 0.1 K noise level.

Radiometer calibrations were made following the chopper-wheel method of Davis and Vanden Bout (1973) with the refinements of Kutner (1978). A chopper-wheel calibration was

[1] Visiting Astronomer, Cerro Tololo Inter-American Observatory, operated by AURA, under contract to the NSF.

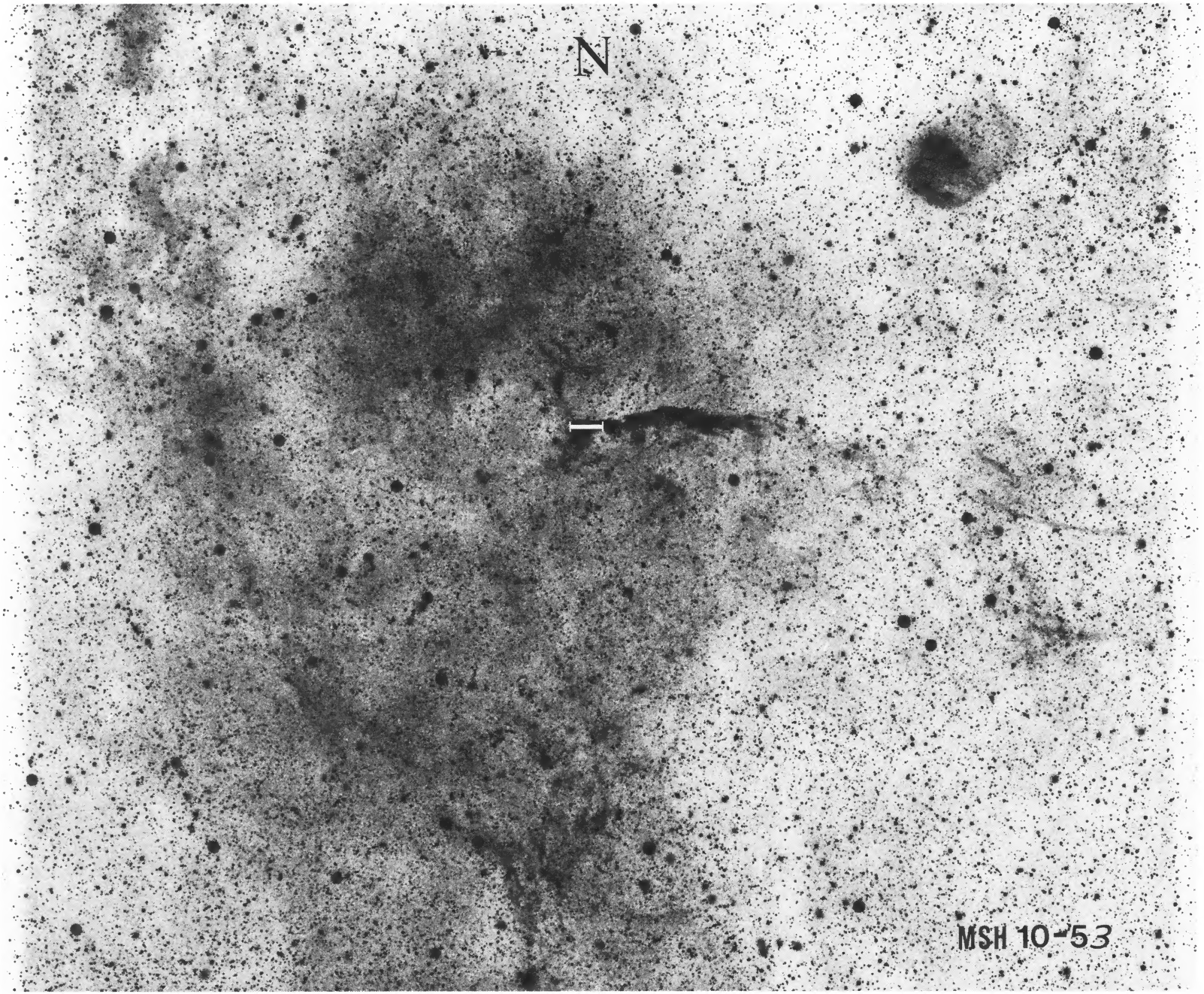

FIG. 1.—Optical filament in MSH 10−53. The position of the slit is indicated over a 2 hr, 098-04, Hα plate obtained at the prime focus of the CTIO 4 m telescope. The length of the bar indicating the position of the extracted spectra is 1′.

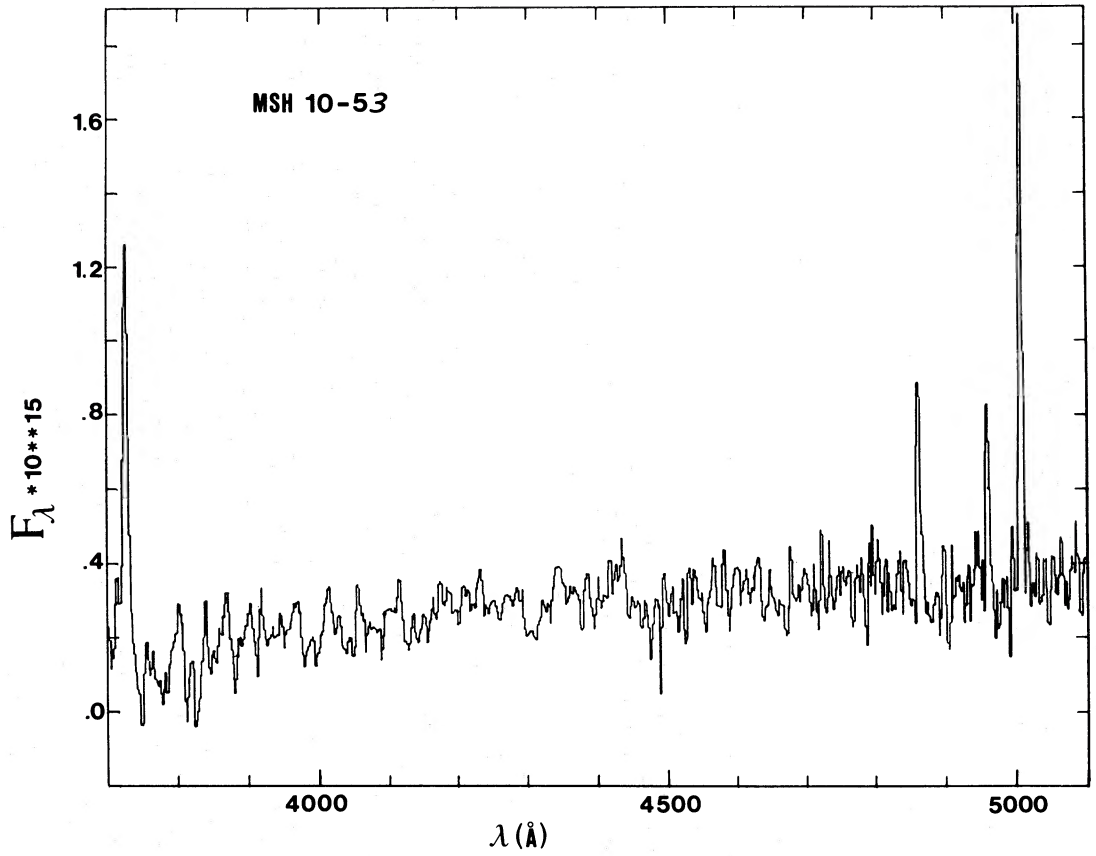

FIG. 2*a*

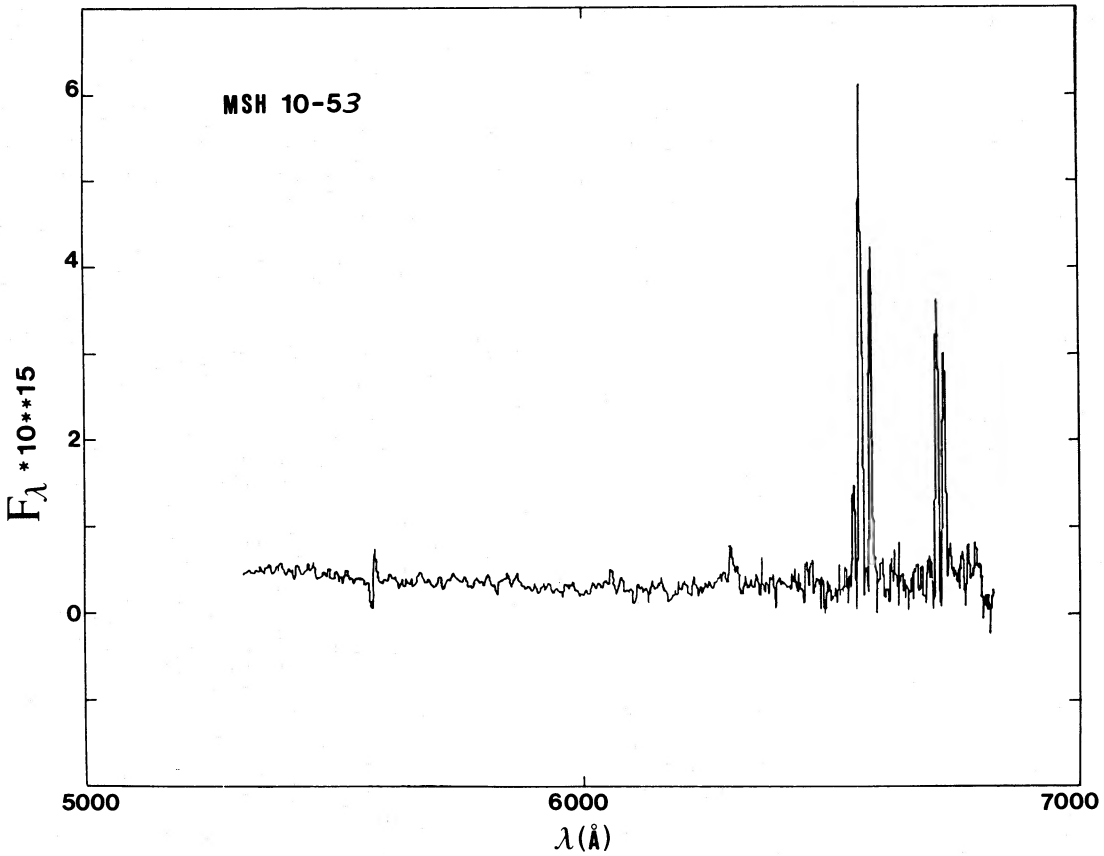

FIG. 2*b*

FIG. 2.—Blue and red spectrograms of the optical filament in MSH 10−53

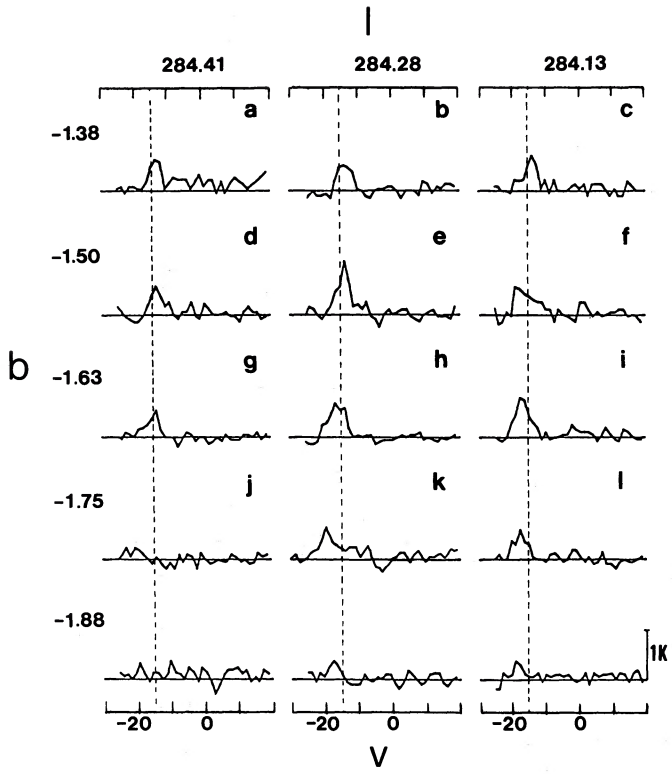

FIG. 3.—Sample of ^{12}CO line profiles observed toward MSH 10−53. Positions in galactic coordinates and radial velocities in km s^{-1} with respect to the local standard of rest are shown. The dashed line at −15 km s^{-1} is included as a reference only to vizualize the velocity gradient between spectra. Labeled spectra are included in Table 2. Line profiles e, k, and f deserve special attention and are discussed in the text.

performed before each integration. Measurements of Orion A allowed a general calibration and system performance monitoring.

All spectra obtained were examined visually and fitted with a linear baseline. If a spectrum showed evidence of a nonlinear baseline, or other baseline irregularity, it was rejected from the observing data base and the corresponding scan was repeated. Several of the spectra taken in the direction of MSH 10−53 are shown in Figure 3. The sampling interval between adjacent scans is 8′.

The basic strategy for the CO observations was to begin mapping near the position of the optical filament and to follow the emission to the 3 σ (0.3 K) noise level, covering most of the region related to the nonthermal radio source MSH 10−53 (Milne 1971).

Data processing and contour maps were made at the telescope site using a Nova 4/× mini computer.

III. RESULTS

Observed line intensities $F(\lambda)$ from the optical filament at the position indicated in Figure 1 are given in Table 1. The observed Hα/Hβ ratio was 14.4; assuming that the unreddened Hα/Hβ ratio is 3, then we get a visual absorption $A_v = 4.4$ mag. The values of $I(\lambda)$ in Table 1 are line intensities corrected for interstellar reddening using the Galactic reddening law derived by Whitford (1958).

The optical spectra suggest that, given the heavy reddening implied by the Hα/Hβ ratio ($A_v = 4.4$ mag), and considering

TABLE 1

LINE INTENSITIES[a]

Identification	$F(\lambda)$	$I(\lambda)$[b]	Model D
[O II] 3727+29	266	1109	915
Hβ 4861	100	100	100
[O III] 4959	76	69	50
[O III] 5007	224	195	150
[O I] 6300	255	66	33
[N II] 6548	290	62	66
Hα 6563	1440	301	321
[N II] 6584	975	204	197
[S II] 6717	871	158	146
[S II] 6731	711	129	120

[a] Hβ = 100.
[b] A_v(mag) = 4.4.

that this is an area of heavy obscuration (>1 mag) beyond 1 kpc (Fitzgerald 1968), the filament is at a distance $d \gtrsim 1$ kpc. On the other hand it cannot lie beyond the near side of the Carina spiral arm, at 2.9 kpc, because in that case one should not expect to see the optical filament that would be buried in large amounts of gas and dust present in the Carina arm.

So optical observations indicate a distance for MSH 10−53 between 1 kpc and 2.9 kpc. Later including the CO observations we will favor a distance of 2.9 kpc a value that considering the errors involved in the different methods is consistent with the 3.5 kpc distance inferred from the Σ-D relation.

Another important result obtained from the line intensities of Table 1 is the shocked emission nature of these lines of the kind expected to arise from a supernova remnant. The Hα/[S II] and Hα/[N II] ratios from Table 1 indicate collisional exitation (Sabbadin and Bianchini 1977), confirming the assumed connection between the optical filament (van den Bergh, Marscher, and Terzian 1973) and the extended nonthermal radio source MSH 10−53.

In Table 1 we also give the line intensities predicted by Shull and McKee (1979) for their model D; these are theoretical models of interstellar radiative shocks, and for model D they took a shock velocity $v_s = 90$ km s^{-1}, a preshock density $n_0 = 10$ cm^{-3}, a preexisting magnetic field of $B_0 = 1$ μG, cosmic metal abundances, and a postshock temperature $T_2 = 1.9 \times 10^5$ K.

The good agreement between the observed line strengths in MSH 10−53 and model D of Shull and McKee suggest that the remnant is relatively old ($\sim 10^4$ yr) and the emitting gas in the optical filament is just interstellar matter of cosmic abundance, swept by the expanding supernova shock wave.

In order to analyze the molecular clouds seen toward MSH 10−53, the observed CO spectra were numerically integrated over velocity, and two-dimensional maps were obtained. A series of contour maps covering the range −25.35 to 15.05 km s^{-1} were visually inspected to explore a possible interaction between the supernova remnant and the molecular clouds. The −21.45 to −14.95 km s^{-1} contour map showed a clear overall correlation with MSH 10−53 (Fig. 4). For comparison only, two isophotes from the 2.7 GHz continuum observation (Milne 1971) have been drawn with broken lines (Fig. 4).

To further investigate this correlation, nine channel maps covering the range −24.05 to −12.35 km s^{-1} were made (Fig. 5). Channel maps at −20.8, −18.2, and −15.6 km s^{-1} show interesting results. At −20.8 km s^{-1} there is a very well defined emission feature at $l = 284.^\circ2$ $b = -1.^\circ7$, just below the

TABLE 2

MAIN PARAMETERS FOR THE SPECTRA SHOWN IN FIGURE 3

Scan	l	b	Δv (km s^{-1})	T_{int}[a] (K km s^{-1})	$\bar{v}$[b] (km s^{-1})	T_{peak} (K)	v_{peak} (km s^{-1})	Equivalent Width[c] (km s^{-1})
a	284°.410	−1°.380	7.4	2.6	−13.8	0.67	−13.3	3.9
b	284.284	−1.380	8.8	2.9	−13.4	0.54	−13.8	5.4
c	284.129	−1.380	8.4	3.2	−14.1	0.72	−13.9	4.4
d	284.410	−1.500	9.6	2.1	−13.1	0.54	−13.3	3.9
e[d]	284.284	−1.505	13.5	4.7	−13.3	1.06	−13.5	4.4
f[e]	284.129	−1.550	13.0	3.6	−15.0	0.51	−18.5	7.0
g	284.410	−1.625	9.3	2.3	−15.2	0.54	−13.6	4.3
h_1	284.265	−1.653	11.2	3.4	−16.3	0.64	−16.4	5.3
h_2	284.284	−1.630	11.2	4.6	−15.7	0.89	−14.8	5.5
i	284.129	−1.675	10.9	4.2	−16.8	0.83	−17.5	5.1
j[g]	284.410	−1.750	...	...	...	...	...	...
k_1	284.210	−1.749	10.0	3.4	−17.5	0.54	−20.1	6.3
k_2[g]	284.265	−1.750	16.1	3.6	−16.5	0.64	−20.1	5.6
k_3	284.284	−1.755	10.8	2.1	−19.6	0.58	−20.1	3.6
l	284.129	−1.803	8.7	2.6	−17.5	0.58	−17.5	4.5

[a] Integrated temperature defined as the antenna temperature (T_A*) integrated over the velocity range of the line (Δv).
[b] Temperature-weighted mean velocity.
[c] Equivalent width defined as the antenna temperature (T_A*) integrated over the velocity range of the line (Δv), divided by the peak antenna temperature of the line.
[d] Highest peak temperature (T_{peak}); fairly large velocity range of the line (Δv); apparent shoulder and fast rise on the right side of the peak.
[e] Highly asymmetric spectral line; largest equivalent width.
[f] Emission below 3 σ.
[g] Largest velocity range (Δv); apparent shoulder and fast rise on the left side of the peak.

center of symmetry of the 2.7 GHz map (Milne 1971), while at −15.6 km s^{-1} there is an even stronger emission at $l = 284°.2$, $b = -1°$ just above the same center. We interpret these features as being located on the supernova remnant shell along the line of sight through the center, one being the closest (approaching us) and the other at the farthest distance (receding from us). The −28.2 km s^{-1} channel map delineates the shell in the lower left side of the 2.7 GHz map similar to what is shown in Figure 4; it also shows an emission point in the upper right side at $l = 284°.1$ $b = -1°.5$.

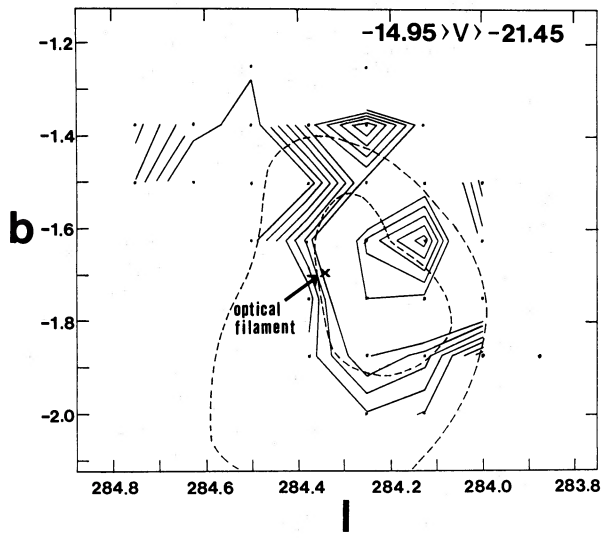

FIG. 4.—^{12}CO contour map of the antenna temperature integrated over the −14.95 to −21.45 km s^{-1} velocity range (LSR). Contour intervals increase in 0.2 K km s^{-1} steps. The positions observed are indicated by dots. Dashed lines correspond to the 2.7 GHz continuum observations of MSH 10−53 (Milne 1972). The close correlation between the CO contour lines with the half-intensity continuum data at the lower and left sides is evident.

Through the analysis of the CO spectra observed (Fig. 3), including a comparison of the shape, velocity of the peak, line width, and integrated temperature, we have been able to obtain additional information confirming the findings provided by the contour maps. Starting with spectrum k ($l = 284°.2$, $b = 1°.7$), we immediately see its rather peculiar shape i.e., an apparent shoulder followed by a fast rise on the left side of the peak. The radial velocity of the peak (−20.1 km s^{-1}) and v_1 (−25.9 km s^{-1}) are the most negative of the region, while the line interval (16.1 km s^{-1}) is the highest. The feature e at $l = 284°.2$, $b = -1°.5$ has a similar shape but with an apparent shoulder and a fast rise on the right side of the peak (−13.5 km s^{-1}); it also has the largest peak (1.06 K) and integrated (4.7 K km s^{-1}) temperatures in the remnant region. The shape of the spectrum f at $l = 284°.1$, $b = -1°.5$ is quite different with a sharp peak on the extreme negative velocity side and a gradual decay in temperature toward the positive side; it has the largest equivalent width (7.0 km s^{-1}) of the mapped area without any evidence of a shoulder.

An interesting result shows up through the comparison of spectra e and k_2 where one looks like the image of the other, that is, the shoulder followed by the sharp peak in e is toward positive velocities, while in k_2 they appear toward the negative side, suggesting a common phenomenon but involving opposite directions, as would be the case for two features on opposite sides of an expanding shell seen along the line of sight through the center of the remnant. Furthermore, if we interpret the peak of the profile to be the shock and the shoulder as the preshock cloud (Elmegreen and Moran 1979) the same picture can be drawn. Thus, altogether the contour maps and the spectra from the CO observations can be interpreted as giving clear evidence of the interaction of the supernova remnant with the surrounding molecular clouds.

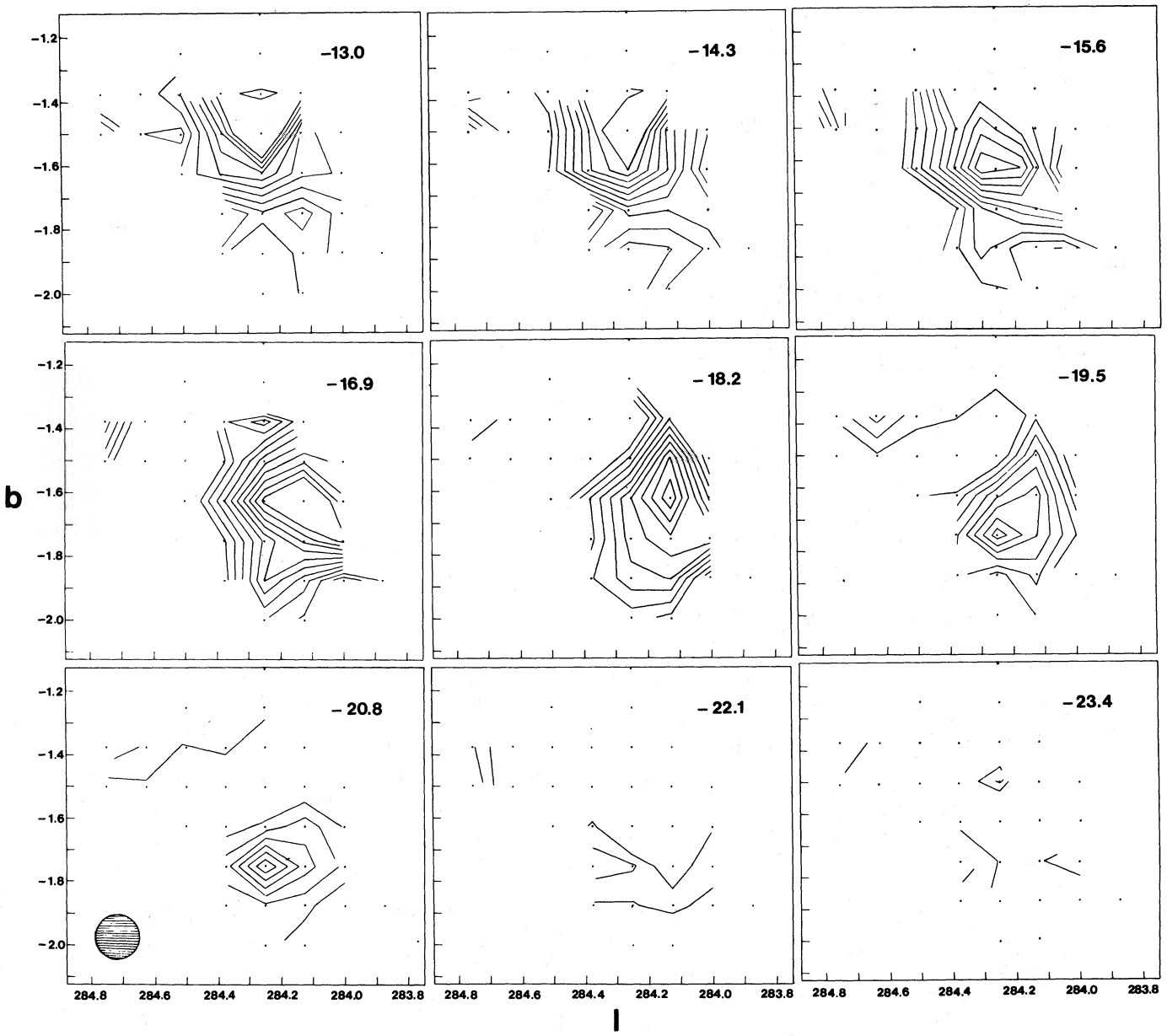

FIG. 5.—^{12}CO channel maps of the MSH 10−53 region from −13.0 km s^{-1} to −23.4 km s^{-1} are shown. The contours increase in steps of 0.15 K km s^{-1}. From maps at −15.6, −16.9, and −18.2 km s^{-1} the shape of a shell can be inferred looking at the contour lines on the lower left part of the plotting area. Features at −20.8 and −15.6 km s^{-1} seems to be part of an expanding shell approaching and receding from us, respectively. The half-power beamwidth of the telescope is shown at the lower left corner.

IV. DISCUSSION

The existence of sudden changes with position in radial velocity and line width of the line profiles from molecular clouds (Slysh *et al.* 1980), and the presence of broad asymmetric lines with a peak-shoulder profile (Elmegreen and Moran 1979; Wootten 1981), have been considered evidence for the interaction of a shock wave with the molecular clouds in the area.

Our CO observations of the MSH 10−53 area show all of the above characteristics. We observe a large difference in the shape of the line profile from one position to the next (see Fig. 4); moreover in position k (see Table 2) we obtained three spectra at positions k_1, k_2, and k_3, separated by one-quarter of a beam, and the shape is quite different for all three of them. In Figure 3 we present k_2 that seems to show more clearly asymmetry due to the shock.

The shell swept by the blast wave is best seen in the contour map of Figure 4, and in Figure 5 at -15.6 km s^{-1} $> v > -18.2$ km s^{-1}, so we take a value of 16.9 km s^{-1} for the shell velocity. The shell is probably formed by the remains of the smaller clouds ($M_c < 10^4$) disrupted by the supernova blast wave (Wheeler, Mazurek and Sivaramakrishnan 1980). The material in the projected shell should have a zero radial velocity component. More massive clouds will survive the explosion. In IC 443 and the Cygnus Loop Scoville *et al.* (1977) found evidence of the existence of these clouds; in Figure 5 we are observing three of them interacting with the supernova

shock. The channel map at $v = -15.6$ km s^{-1} shows the interaction between a cloud and the supernova shock in the far side of the expanding wave, with a small positive velocity compared with the shell velocity $v = 16.9$ km s^{-1}, which can be explained by the fact that the shock receding from us will encounter resistence to its expansion because it is moving inward into the Carina spiral arm, while the clouds seen at $v = -18.2$ km s^{-1} and $v = -20.8$ km s^{-1} have larger negative velocities because they are located in the near side of the spherical shock and expanding away from the spiral arm into a medium of ever-decreasing density. This scenario is also suggested by the shape of the spectra e and k of Figure 3, as described in § III.

From our optical and CO observations we conclude that MSH 10−53 correspond to the remnant of a supernova that exploded some 10^4 yr ago at 2.9 kpc from us in the Carina spiral arm. A distance of 2.9 kpc for the near side of the Carina arm has been taken considering the radial velocity of −16.9 km s^{-1} observed in the CO line from the projected remnant shell. From Cohen *et al.* (1985) one can get a radial velocity of −19 km s^{-1} for the η Car nebula, at a distance of 2.7 kpc and at $l = 287°.5$, thus MSH 10−53 with a larger radial velocity component and at a longitude $l = 284°.4$ should be located at a slightly larger distance. Given its location inside a spiral arm, the supernova was most likely a Type II with a massive stellar progenitor.

In the past ($\sim 10^4$ yr ago), right after the explosion the supernova remnant was probably observable as an IR source, due to the absorption and reemission of the energy from the explosion, by the grains in the surrounding medium (Shull 1980; Wheeler, Mazurek, and Sivaramakrishnan 1980). At present we can see the effect of the blast wave upon the molecular clouds which have been accelerated, disrupted, and swept by the supernova shock. We also established the presence of at least one optical filament which represents shocked intercloud material swept by the supernova blast wave and blown through a "hole" in the molecular cloud complex.

One small additional piece of evidence of the effect of this supernova explosion upon its surrounding medium can be seen in the longitude-velocity diagram of Figure 1 (*left*) of Cohen *et al.* (1985), where we see a hole in the position of MSH 10−53 ($l \approx 284.3$, $v \approx -18$ km s^{-1}) due to the lack of material at the local velocity, material that could have been accelerated by the supernova blast wave. It is quite reasonable to suspect that some of the observed anomalies, in the data from molecular clouds used to determine the rotation curve of the Galaxy, would be partly due to the influence of supernova shocks that disturb the local velocity field.

An optical search for more filaments belonging to the remnant will be very helpful. Given the large amounts of H II regions in the area, the best way of selecting possible filaments would be to obtain interference-filter plates of the area and look for shocked material.

It would also be interesting to check whether, as in W28 and W44 (Wootten 1981), one can find OH masers in places where the supernova shock is interacting with molecular clouds.

It has been found that the chemical composition of a molecular cloud affected by a shock is different than that of the typical interstellar cloud (DeNoyer and Frerking 1981). Thus further evidence of the interaction of MSH 10−53 with the surrounding clouds could be obtained from an abundance study of the shocked molecular clouds.

This research was partially supported by the grants from DIB (Universidad de Chile) number E 1706-8533 (M. T. R.) and E 2242-8512 (J. M.).

One of the authors (J. M.) is specially grateful to Professor Patrick Thaddeus and Dr. Richard S. Cohen for giving him the opportunity of participating in the Columbia Southern Hemisphere Millimeter Project financed by a National Science Foundation grant.

REFERENCES

Cohen, R. S. 1983, in *Surveys of the Southern Galaxy*, ed. W. B. Burton and F. P. Israel (Dordrecht: Reidel), p. 265.
Cohen, R. S., Grabelsky, D. A., May, J., Bronfman, L., Alvarez, H., and Thaddeus, P. 1985, *Ap. J. (Letters)*, **290**, L15.
Cornett, R. H., Chin, G., and Knapp, G. R. 1977, *Astr. Ap.*, **54**, 889.
Davis, J. H., and Vanden Bout, P. 1973, *Ap. Letters*, **15**, 43.
De Noyer, L. K., and Frerking, M. A. 1981, *Ap. J. (Letters)*, **246**, L37.
Elmegreen, B. G., and Moran, J. M. 1979, *Ap. J. (Letters)*, **227**, L93.
Fitzgerald, M. P. 1968, *Ap. J.*, **73**, 983.
Herbst, W., and Assousa, G. R. 1977, *Ap. J.*, **217**, 473.
Kutner, M. L. 1978, *Ap. Letters*, **19**, 81.
Mills, B. Y., Slee, O. B., and Hill, E. R. 1961, *Australian J. Phys.*, **14**, 497.
Milne, D. K. 1971, in *IAU Symposium 46, The Crab Nebula*, ed. R. D. Davies and F. G. Smith (Dordrecht: Reidel), p. 248.
———. 1972, *Australian J. Phys.* **25**, 307.
Milne, D. K., and Dickel, J. R. 1975, *Australian J. Phys.*, **28**, 209.
Sabbadin, F., and Bianchini, A. 1977, *Astr. Ap.*, **55**, 177.
Scoville, N.Z., Irvine, W. M., Wannier, P. G. and Predmore, C. R. 1977, *Ap. J.*, **216**, 320.
Shull, J. M. 1980, *Ap. J.*, **237**, 769.
Shull, J. M., and McKee, C. F. 1979, *Ap. J.*, **227**, 149.
Slysh, V. I., Wilson, T. L., Pauls, T., and Henkel, C. 1980, in *IAU Symposium 87, Interstellar Molecules*, ed. B. H. Andrew (Dordrecht: Reidel), p. 473.
van den Bergh, S., Marscher, A. P., and Terzian, Y. 1973, *Ap. J. Suppl.*, **26**, 19.
Wheeler, J. C., Mazurek, T. J., and Sivaramakrishnan, A. 1980, *A.J.*, **237**, 781.
Whitford, A. E. 1958, *A.J.*, **63**, 201.
Wootten, A. 1981, *Ap. J.*, **245**, 105.

JORGE MAY and MARÍA TERESA RUIZ: Departamento de Astronomía, Universidad de Chile, Casilla 36-D, Santiago, Chile